PROTEINS
STRUCTURE ■ FUNCTION ■ BIOINFORMATICS

Structural origins of pH-dependent chemical shifts in the B1 domain of protein G

Jennifer H. Tomlinson, Victoria L. Green, Patrick J. Baker, and Mike P. Williamson*

Department of Molecular Biology and Biotechnology, University of Sheffield, Firth Court, Western Bank, Sheffield, S10 2TN, United Kingdom

ABSTRACT

We report chemical shifts for H^N, N, and C′ nuclei in the His-tagged B1 domain of protein G (GB1) over a range of pH values from pH 2.0 to 9.0, which fit well to standard pH-dependent equations. We also report a 1.2 Å resolution crystal structure of GB1 at pH 3.0. Comparison of this crystal structure with published crystal structures at higher pHs provides details of the structural changes in GB1 associated with protonation of the carboxylate groups, in particular a conformational change in the C-terminus of the protein at low pH. An additional change described recently is not seen in the crystal structure because of crystal contacts. We show that the pH-dependent changes in chemical shifts can be almost entirely understood based on structural changes, thereby providing insight into the relationship between structure and chemical shift. In particular, we describe through-bond effects extending up to five bonds, affecting N and C′ but not H^N; through-space effects of carboxylates, which fit well to a simple electric field model; and effects due to conformational change, which have a similar magnitude to many of the direct effects. Finally, we discuss cooperative effects, demonstrating a lack of cooperative unfolding in the helix, and the existence of a β-sheet "iceberg" extending over three of the four strands. This study therefore extends the application of chemical shifts to understanding protein structure.

Proteins 2010; 78:3000–3016.

Key words: NMR chemical shift; structural change; protonation; electric field effect; conformational change; cooperative hydrogen bonding; *Staphylococcal* protein G.

INTRODUCTION

Chemical shifts have long been of interest to structural biologists because their dependence on the chemical environment of the atom means they contain a wealth of structural information. However, the complex nature of the influences on chemical shifts has limited their use historically for structure determination, leading to a greater dependence on the NOE and other measurements. Knowledge of chemical shifts has advanced over recent years, with programs such as SHIFTX[1] and total[2] allowing fairly accurate calculations of chemical shifts from known structures. This and further elucidation of the influences on chemical shifts have led in recent years to a resurgence in interest in chemical shifts, with several groups investigating the use of chemical shifts directly in structure determination.[3–6] Nevertheless, the detail of the relationship between structure and shift has not yet been determined well enough for direct structure determination from chemical shifts.

Although chemical shifts remain too complex for detailed structural analysis, changes in chemical shifts can provide useful information on changes in structure upon changes in the environmental conditions of a protein and can often be meaningfully interpreted.[7,8] We have therefore focused on changes in chemical shift and their relationship to structure.

pH-dependent changes in chemical shift can provide a lot of information, particularly with regard to hydrogen bonding involving charged side chains.[9–12] Amides that form hydrogen bonds to carboxylate side chains show large pH-dependent changes in proton shift in response to the protonation of that side chain of up to 1 ppm.[9] Such an effect has also been observed in bull seminal inhibitor IIA[10] and *Bacillus agaradhaerens* xylanase[12] as well as Sac7d and Sso7d.[11] Betz *et al.*[12] also found evidence of the titration of one side chain influencing the chemical shifts of another titrating side chain via an intermediate residue that forms hydrogen bonds with both side chains. This indicates that the effect of such titrations on chemical shifts can be propagated through hydrogen bond networks.

Amide proton shifts have been shown to shift upfield upon deprotonation of a carboxylate (i.e., with increased pH) when the amide in question is affected by interactions mediated through covalent bonds[13]: this is what Bundi and Wüthrich[9] called an "intrinsic titration shift." In addition, the chemical shift of amide protons that hydrogen bond to

*Correspondence to: Mike P. Williamson, Department of Molecular Biology and Biotechnology, University of Sheffield, Firth Court, Western Bank, Sheffield, S10 2TN, UK. E-mail: m.williamson@sheffield.ac.uk
Received 27 April 2010; Revised 28 June 2010; Accepted 6 July 2010
Published online 23 July 2010 in Wiley Online Library (wileyonlinelibrary.com).
DOI: 10.1002/prot.22825

carboxylate side chains has been observed to shift upfield with reduced pH, whereas those that are affected by through-space electrostatic interactions shift downfield.[11] The magnitude of the pH-dependent chemical shift change for these amides has been related to the hydrogen bond strength, stronger hydrogen bonds causing a greater chemical shift change.[14]

The pH dependence of amide nitrogen chemical shifts in the backbone of *Bacillus agaradhaerens* xylanase, some of which did not form hydrogen bonds with titrating side chains, were found to be dependent on nearby aspartate and glutamate side chains,[12] some of which were rationalized in terms of side chain rearrangements and alterations in the hydrogen bonding network.[12] This implies that pH-dependent chemical shift changes can provide information about long-range interactions.

Studies of the changes in carbon chemical shifts in amino acids with pH have identified a through-bond effect, which decreases with increased separation from the protonation site in the titrating side chain.[15–18] However, the magnitude of the protonation shift also depends on the polarizability of the atom, and is therefore larger at the carbonyl carbon than expected by this trend, because carbonyl carbons are more polarizable.

The analysis of chemical shift changes with pH is often hampered by a lack of detailed structural information at different pHs that can then be related to the chemical shift changes observed. In this study, the structure of an N-terminally His-tagged form of the *Staphylococcal* protein G B1 domain (GB1) at pH 3.0 was determined at 1.2 Å resolution by X-ray crystallography, allowing a comparison between this model and previously published crystal structures[19] determined at pH 4.0 and 4.5 (PDB IDs 1pgb and 1pga, respectively). In a recent publication (Tomlinson *et al.*, 2010),[20] we have also characterized a pH-dependent structural change at the C-terminus of the helix, which is not seen in the crystal structure because of crystal contacts. Together, these details of the low-pH structure allow chemical shift changes to be related to changes in structure in response to the titration of carboxylate side chains.

We have previously reported pK_a values for all the lysine, aspartate, and glutamate residues in GB1[21] (except E50, the pK_a of which was previously determined by Khare *et al.*[22]) and these are reproduced in Table I. These pK_as are used here to identify the titrating groups that are the origins of the pH-dependent chemical shift changes reported here.

Here, we analyze the pH-dependent chemical shift changes in GB1, and relate them to specific titrating groups. We show how chemical shifts are affected by through-bond effects, by direct through-space electrostatic effects, and by conformational change, all of which are significant. We also show that chemical shifts can be used to characterize cooperative changes in structure, and therefore provide information on dynamic behavior.

Table I
The pK_as of the Carboxylate and Lysine Residues in GB1 Reported Previously in 100 m*M* Salt, 90% H_2O, 10% D_2O, 298 K[21,22]

Residue	pK_a determined in previous study[21]
D9	3.24 ± 0.01
E23	4.37 ± 0.01
E27	4.16 ± 0.01
D30	2.78 ± 0.01
E35	4.56 ± 0.04[a]
D44	3.75 ± 0.01
D48	4.03 ± 0.01
E50	4.4 ± 0.1[b]
D54	3.93 ± 0.01
D55	3.24 ± 0.01
E64/C-terminus[c]	3.23 ± 0.03 and 4.51 ± 0.04[c]
K12	10.7 ± 0.04
K18	11.1 ± 0.1
K21	11.4 ± 0.1
K36	10.8 ± 0.1
K39	11.1 ± 0.1
K58	11.4 ± 0.1

The uncertainties reported here are the uncertainties in the fitting of the experimental data to a single pK_a value. The error in the pK_a value is larger because of errors in pH meter calibration etc, but probably by no more than 0.03.
[a]With a Hill coefficient of 0.84. For all other residues the Hill coefficient was 1.0.
[b]Not determined by Tomlinson *et al.*[21] as the peak became broad and overlapped at low pH and could not be identified accurately but determined previously by Khare *et al.*[22]
[c]The data do not unambiguously permit a distinction between these two since E64 is the C-terminal residue. However, magnitudes of shifts at different nuclei suggest that the side chain has the pK_a of 3.23.
The lysine pKas are only determined approximately as the unfolding of the protein at high pH prevented the observation of complete titrations. GB1 does not contain any histidines except that the construct used in this study retained an N-terminal histidine tag, MH6AMD. The N-terminus is expected to have a pKa of ~8, based on literature values.

MATERIALS AND METHODS

Protein expression and purification and sample preparation

The protein G B1 domain (GB1) was expressed as a His-tagged construct with the sequence MH_6AMD preceding the normal N-terminal sequence from a gene inserted into a pET-15b vector. Residues are numbered from 1 at the first histidine, making the C-terminus (residue 324 of the mature protein) residue 64. This is the same numbering scheme as in our previous work,[20,21] and is 8 larger than the most common numbering scheme. The protein was expressed in *Escherichia coli* BL21 (DE3) pLysS cells grown at 37 °C either in M9 minimal medium containing 1.5 g/L ^{13}C-glucose, 1 g/L ^{15}N-amonium sulfate as described previously,[21,23] or in LB medium. Expression was induced with 1 m*M* IPTG overnight at 25 °C after an $OD_{280\ nm}$ of 0.6 was reached. The protein was purified using a nickel affinity column (HIS-select nickel affinity gel, Sigma-Aldrich) followed by gel filtration in 50 m*M* potassium phosphate buffer plus 150 m*M* NaCl and 1 m*M* sodium azide, pH 6.0. Buffer exchange and protein concentration was carried out in vivaspin centrifugal concentrators (Sartorius).

GB1 samples for NMR experiments (1 m*M* and 310 μ*M*) were produced in a buffer containing 33 m*M* so-

dium phosphate, 33 m*M* deuterated sodium acetate, 33 m*M* orthoboric acid (which was substituted with 33 m*M* sodium citrate for samples below pH 4.0), 1 m*M* sodium azide, and 10% deuterium oxide. Sample pH was altered by buffer exchange with freshly prepared buffer at the desired pH to prevent an increase in salt concentration during the titration. GB1 samples (1 m*M* ^{13}C, ^{15}N) were used for all spectra except the CBCA(CO)NH for which a 310 μ*M* ^{13}C, ^{15}N protein sample was used.

For crystallization trials, a protein stock solution of 20 mg/mL unlabelled GB1 in 50 m*M* tris-HCl, pH 6.0 was prepared.

NMR experiments and data processing

All spectra except the HSQC-NOESY and HSQC-TOCSY spectra were acquired using a Bruker DRX 600 MHz spectrometer fitted with a cryoprobe and were recorded at 298 K. The HSQC-NOESY and HSQC-TOCSY spectra were acquired using a Bruker DRX 600 MHz spectrometer at 298 K without a cryoprobe. Spectra were processed using Felix (Felix NMR Inc.) and data were analyzed using home written scripts running under Linux.

Amide proton and nitrogen chemical shifts were measured using HSQC spectra recorded every 0.25 pH units from pH 2.0 to 6.0 and every 0.5 pH units from pH 6.0 to 9.0. Carbonyl carbon chemical shifts were measured using 2D HNCO spectra in which the nitrogen frequency labeling was omitted. These spectra were acquired at the same pHs as the HSQC spectra above.

HSQC spectra at pH 5.0 were assigned by comparison with previously published assignments[23] and subsequent spectra were assigned by tracking the movement of peaks between spectra. HSQC spectra at pH 3.0, however, could not be assigned unambiguously using this method so HSQC-NOESY and HSQC-TOCSY spectra were acquired and used to assign resonances at pH 3.0 by comparison with the previously published side chain assignments.[23] The HSQC-TOCSY spectrum was acquired using a 300 μ*M* ^{15}N-labeled GB1 sample with a mixing time of 35 ms, whereas the HSQC-NOESY spectrum was acquired using the same sample with a mixing time of 150 ms. Finally, these pH 3.0 assignments were confirmed using a CBCA(CO)NH spectrum recorded on a 500 MHz Bruker DRX spectrometer with a 1 m*M* ^{13}C and ^{15}N labeled GB1 sample at pH 3.0 with reference to previously published assignments.[23]

HNCO spectra were assigned at pH 5.0 by reference to the previously published assignments[23] and spectra at subsequent pHs were assigned by tracking the movements of these peaks. Because of large shift changes at low pH, some assignments in crowded regions required comparison with reassigned signals at pH 3.0.

pH dependent chemical shift fitting

Chemical shift changes with pH were fitted to the following equations describing dependence on one,[22] two, or three[24] pK_as, or one pK_a and a Hill coefficient different from unity[25] [Eqs. (1–4), respectively].

$$\delta = \frac{\delta_{acid} + \delta_{base}10^{(pH-pK_a)}}{1 + 10^{(pH-pK_a)}} \quad (1)$$

$$\delta = \frac{\delta_a 10^{-2pH} + \delta_b 10^{-(pH-pK_{a1})} + \delta_c 10^{-(pK_{a1}-pK_{a2})}}{10^{-2pH} + 10^{-(pH-pK_{a1})} + 10^{-(pK_{a1}-pK_{a2})}} \quad (2)$$

$$\delta = \frac{\delta_a 10^{-3pH} + \delta_b 10^{-(pK_{a3}+2pH)} + \delta_c 10^{-(pK_{a2}+pK_{a3}+pH)} + \delta_d 10^{-(pK_{a1}+pK_{a2}+pK_{a3})}}{10^{-3pH} + 10^{-(pK_{a3}+2pH)} + 10^{-(pK_{a2}+pK_{a3}+pH)} + 10^{-(pK_{a1}+pK_{a2}+pK_{a3})}} \quad (3)$$

$$\delta = \frac{\delta_{acid} + \delta_{base}10^{n(pH-pK_a)}}{1 + 10^{n(pH-pK_a)}} \quad (4)$$

Fitting was carried out using a Levenberg-Marquardt least squares routine. *F* tests were carried out to determine which equation gave the best fit to the data, the simplest equation that gave a good fit to the data being chosen. Models with larger numbers of variables were only used if the improvement in fit was statistically significant.

The pK_as influencing these chemical shift changes (described below as pK^{app}) were then compared with the pK_as of the aspartate and glutamate residues in GB1, determined previously.[21,22] To aid analysis, total chemical shift changes of 0.1 (proton), 0.5 (nitrogen), and 0.2 ppm (carbonyl carbon) were applied as cut-offs below which any change in chemical shift with pH was considered insignificant for the purpose of this study.

Crystallization and crystal structure determination

Crystals were grown by suspending 1 μL drops of 20 mg/mL GB1 in 50 m*M* tris-HCl and 1 μL mother liquor over 1 mL wells of 50 m*M* sodium citrate buffer, 3.8*M* sodium formate, and 8% v/v isopropanol, pH 5.5. Crystals were obtained after 2 weeks with the approximate dimensions 100 μm by 150 μm. A single crystal was subsequently soaked in a solution of 50 m*M* sodium citrate buffer, 3.8*M* sodium formate, and 8 % v/v isopropanol, pH 3.0 for 90 minutes to adjust the pH of the crystal to pH 3.0. When compared with ligand binding studies,

Table II
Data Collection Statistics for the 1.2 Å pH 3.0 Crystal Structure

Data collection statistics	
Resolution (Å)	30.15–1.20 (1.26–1.20 Å)[a]
Unit cell dimensions:	
a	34.8 Å
b	34.8 Å
c	71.8 Å
α	90°
β	90°
γ	120°
Number of observations	108199 (8705)
Number of unique reflections	29246 (3333)
Redundancy	3.7 (2.6)
I/σ	18.5 (2.8)
R_{merge}	0.04 (0.32)
Completeness (%)	96.0 (75.0)

[a]Numbers in parentheses indicate values in the highest resolution shell.

such a length of time should be more than sufficient to allow for buffer diffusion into the crystal.[26,27] We can be confident that the crystal was at pH 3.0 during the diffraction experiment.

X-ray diffraction data were collected at the Diamond synchrotron to 1.2 Å resolution. Data were indexed using MOSFLM[28] to the space group $P3_2$ with the unit cell dimensions shown in Table II with two molecules in the asymmetric unit and subsequently processed using the CCP4 suite of programs.[29] The data were scaled and merged using SCALA[30] and the structure was solved using molecular replacement with the program AMoRe[31] and using the published pH 4.5 crystal structure[19] (PDB ID 1pga) as the initial search model. Refinement was performed using Refmac5[32] and model building using Coot,[33] to produce a final model with an *R* factor of 0.15 and R_{free} of 0.18 (Table III).

RESULTS

pH-dependent chemical shift changes

Changes in backbone amide proton, nitrogen, and carbonyl carbon chemical shifts over the pH range 2.0–9.0 were fitted to equations describing the influence of 1, 2, or 3 pK_as or 1 pK_a plus a Hill coefficient different from 1.0 (Fig. 1), to yield values of apparent p*K*, described here as pK^{app}, for each nucleus with a significant pH-dependent shift. Table IV shows the significant pH-dependent changes in amide proton and nitrogen and carbonyl carbon chemical shifts of each residue in His-tagged GB1. Throughout this article, amide nitrogen and proton, and carbonyl carbon, always refer to backbone atoms unless specifically indicated otherwise. Titration shifts have been added to the TitrationDB database (http://enzyme.ucd.ie/Titration_DB).

Crystal structure at pH 3.0

Overall, the electron density map shows strong, clear density for most residues, as shown in Figure 2, allowing the determination of a clear structure model to a resolution of 1.2 Å, which has been deposited with the Protein Data Bank, www.rcsb.org, with code 3MP9. As in the previously published structures of GB1,[19,34–39] the monomer consists of a four stranded β-sheet composed of two central parallel strands and two outer antiparallel strands packed against an α-helix. The histidine tag, which was not removed from the protein before crystallization, is partially visible in the crystal structure, extending from the N-terminus of the protein in a similar orientation to β-strand 1, as shown in Figure 3.

Some regions, such as the β1-β2 loop, have weaker electron density than the remainder of the molecule, indicating more disordered regions of the protein. These disordered areas are found in places in the structure where more flexibility is expected, such as the N-terminus of the histidine tag, the flexible loops between β-strands 1 and 2 and between the α-helix and the β-strand 3, and the tips of long and flexible side chains, such as those of lysine and carboxylic acid side chains, and probably indicate real areas of disorder rather than deficiency in the data. Indeed, previous ^{15}N relaxation data have shown these two loops to be the most flexible regions of the molecule.[40] However, although weaker, the electron density is sufficient to allow the loops to be modeled accurately into the electron density.

The pH 3.0 structure contains two monomers in the asymmetric unit, packed together through contacts involving the final turn of the α-helix in each chain, as shown in Figure 3. This packing involves an interaction between the D44 side chains in each monomer (see inset in Fig. 3), which would not normally be expected to occur because of repulsion between the two negative charges. However, the pK_a of D44 is 3.75,[21,22] showing that at pH 3.0, the D44 side chain is expected to be protonated so this repulsion would not occur, allowing the formation of a hydrogen bond. This observation therefore further supports our contention that the crystallization pH was genuinely 3.

There are very few differences between the structures of the two chains in the asymmetric unit. No significant differences are observed in backbone conformation and only a small number of side chains have different orientations

Table III
Refinement Statistics for the 1.2 Å Crystal Structure Determined at pH 3.0

Refinement statistics	
Resolution (Å)	30.15–1.20
Unique Reflections	27757
R_{cryst}	0.15
R_{free}	0.18
RMS bond length (Å)	0.010
RMS bond angle (degrees)	1.2
Number of protein atoms	985
Number of water molecules	192
Average temperature factor:	
Protein atoms	20.6
Water molecules	15.0

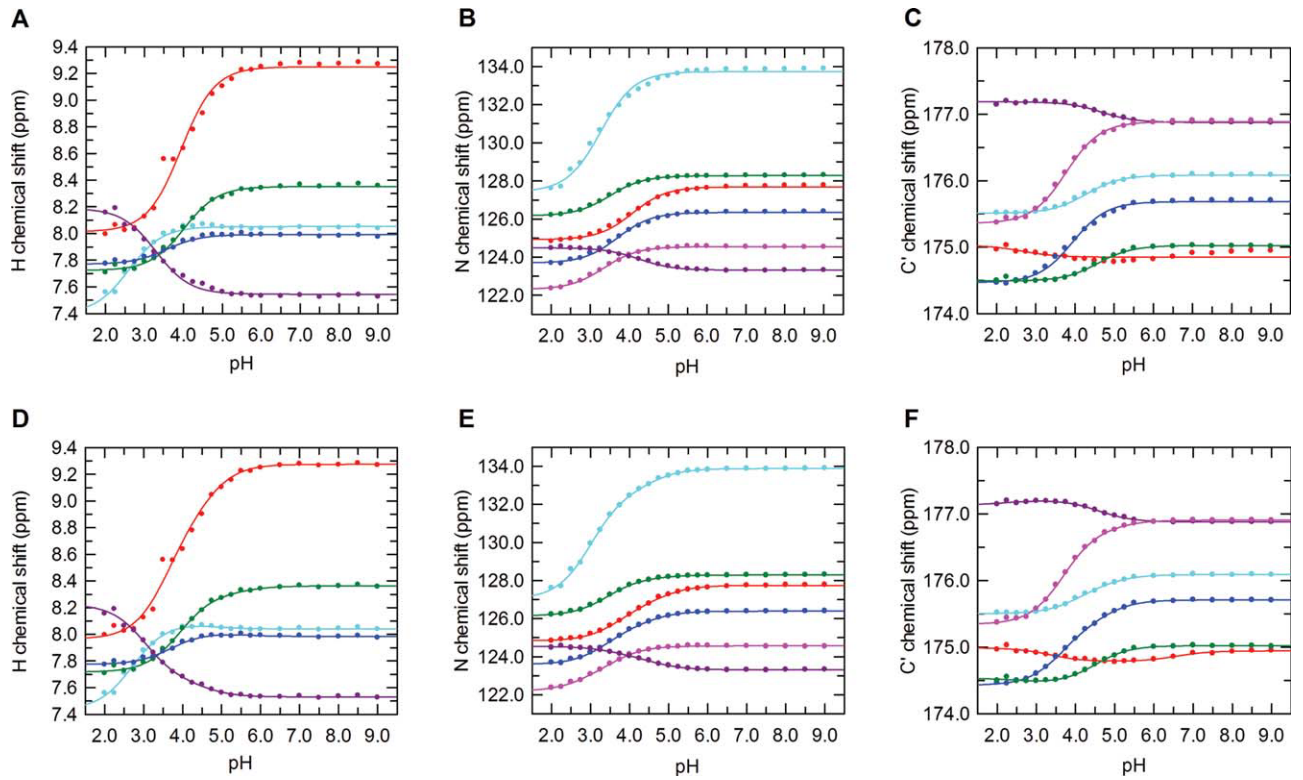

Figure 1

Fits of chemical shift changes with pH to (**A**, **B**, and **C**) one and (**D**, **E**, and **F**) two pK_as. (A and D) amide proton shifts of K18 (red), T33 (cyan), D48 (green), A56 (blue), and E64 (purple). (B and E) amide nitrogen shifts of N16 (blue), D48 (red), D54 (green), D55 (magenta), V62 (purple), and E64 (cyan). (C and F) carbonyl chemical shifts of M8 (red), N16 (blue), E23 (green), E27 (cyan), A34 (purple), and D44 (magenta).

in the two monomers. These are residues such as lysines and carboxylic acid residues that are expected to have more mobile side chains, and therefore, the differences in conformation probably indicate mobile side chains that move between the two conformations. The quality of the electron density for these residues supports this hypothesis as those residues with differing side chain conformations between the two monomers have weaker electron density.

In this article, we compare NMR data with crystal structures. The two are remarkably consistent, despite the fact that crystal structures (including this one) are typically determined in very high salt, which might tend to disrupt hydrogen bonds. It is also worth pointing out that the pH values used for crystallisation (3.0 here and 4.0/4.5 for 1pgb and 1pga) are close to several of the side chain pK_a values, implying that several side chains will be partially deprotonated/protonated. Nevertheless, as discussed below, the state observed in the crystal looks very much like the major protonation state at that pH.

Comparison of pH 3.0 and pH 4.5 crystal structures

The pH 3.0 crystal structure is very similar to the pH 4.5 1pga and the pH 4.0 1pgb crystal structures determined by Gallagher *et al.*,[19] as shown by the overlay of the crystal structures in Figure 4(a). The RMSD between the pH 3.0 and 1pga structures is 0.36 Å and between the pH 3.0 and 1pgb structures is 0.30 Å for all atoms in the protein. The backbone of the α-helix and all four β-strands are very similar in all structures, with the β2 strand showing the largest difference at pH 3.0. The loops show more differences between the structures, with the β1-β2 loop showing a change of 0.7–0.9 Å between the pH 4.0 1pgb structure[19] and the pH 3.0 structure described here. No large changes in the structure of the protein backbone were observed but small changes in the positions of the backbone atoms can lead to differences in hydrogen bonding, which is the main influence on amide proton chemical shifts, and so could explain some of the chemical shift changes between high and low pH discussed later.

The most striking difference in the pH 3.0 structure is that in the 1pga and 1pgb structures,[19] the E64 side chain is inserted between the loops connecting β-strands 1 and 2 and connecting the α-helix and β-strand 3, forming hydrogen bonds with the amides of K18 and D48. In contrast, the pH 3.0 structure has weak electron density for E64, suggesting the residue is not well ordered. At pH 3.0, E64 occupies a different conformation,

Table IV
The pH-Dependent Changes in Amide Proton and Nitrogen and Carbonyl Carbon Chemical Shifts in His-Tagged GB1 within the pH Range 2.0–9.0

Residue	H^n Shift Change pK^{app}	H^n Shift Change Hill Coefficient	H^n Shift Change Magnitude[a] (ppm)	N^h Shift Change pK^{app}	N^h Shift Change Hill Coefficient	N^h Shift Change Magnitude (ppm)	C′ Shift Change pK^{app}	C′ Shift Change Hill Coefficient	C′ Shift Change Magnitude (ppm)
A7	6.58 ± 0.42[b]	0.43 ± 0.12	−0.29	4.17 ± 0.05[b]	0.48 ± 0.03	−1.78	7.00 ± 0.22[c]	1	−0.21
M8	3.63 ± 0.16[d]	1	−0.19	6.43 ± 0.04, 3.86 ± 0.13, and 2.73 ± 0.25[e]	1	−0.57, +0.85, and +1.02	3.37 ± 0.14[d]	1	−0.20
D9	–	–	–	–	–	–	3.18 ± 0.04[d]	1	+0.91
T10	3.17 ± 0.18[d]	1	+0.18	–	–	–	3.85 ± 0.10[b]	0.62 ± 0.07	+0.48
Y11	3.86 ± 0.17[f]	1	+0.13	3.46 ± 0.08[b]	0.67 ± 0.05	+0.77	4.10 ± 0.06[b]	1.42 ± 0.24	−0.29
K12	–	–	–	4.19 ± 0.10[f]	1	+1.13	4.24 ± 0.05[f]	1	−0.42
L13	–	–	–	4.37 ± 0.01[f]	1	+1.51	–	–	–
L15	4.04 ± 0.15[f]	1	+0.15	–	–	–	3.50 ± 0.15[g]	0.73 ± 0.14	−0.31
N16	3.70 ± 0.12[f]	1	+0.19	3.63 ± 0.01[b]	0.77 ± 0.01	+2.90	3.86 ± 0.03[b]	0.76 ± 0.03	+1.31
G17	–	–	–	4.35 ± 0.05[f]	1	+0.50	3.77 ± 0.08[b]	0.68 ± 0.07	+0.55
K18	3.48 ± 0.09 and 4.69 ± 0.13[h]	1	+0.82 and +0.50	3.67 ± 0.04 and 4.83 ± 0.07[i]	1	+1.85 and +1.06	3.70 ± 0.04[b]	0.72 ± 0.04	+1.02
T19	3.52 ± 0.29 and 4.56 ± 0.55[h]	1	+0.37 and +0.18	–	–	–	–	–	–
L20	–	–	–	3.73 ± 0.08 and 4.82 ± 0.16[j]	–	+1.16 and +0.53	3.35 ± 0.06[b]	0.67 ± 0.04	−1.02
K21	3.75 ± 0.31[b]	0.61 ± 0.20	−0.18	3.85 ± 0.07[b]	0.72 ± 0.07	−0.54	3.96 ± 0.11[f]	1	+0.21
G22	–	–	–	–	–	–	3.46 ± 0.18[b]	0.56 ± 0.08	−0.45
E23	–	–	–	4.51 ± 0.03[f]	1	−0.70	4.57 ± 0.04[f]	1	+0.58
T24	–	–	–	4.40 ± 0.02[f]	1	−1.31	–	–	–
T26	–	–	–	–	–	–	4.08 ± 0.22[b]	0.51 ± 0.11	+0.30
E27	–	–	–	4.15 ± 0.02[b]	0.85 ± 0.03	+1.51	4.26 ± 0.04[f]	1	+0.56
V29	–	–	–	–	–	–	2.66 ± 0.21[g]	0.72 ± 0.11	−0.67
D30	–	–	–	2.79 ± 0.02[f]	1	+2.89	2.38 ± 0.05[f]	1	+1.11
A31	2.53 ± 0.29[f]	1	−0.15	2.56 ± 0.04[f]	1	−1.05	2.74 ± 0.14[f]	1	−0.26
A32	2.98 ± 0.36[d]	1	+0.14	4.29 ± 0.03[b]	0.70 ± 0.03	+1.29	2.66 ± 1.16[b]	0.43 ± 0.19	−0.27
T33	2.72 ± 0.09[d]	1	+0.65	2.64 ± 0.03[b]	0.81 ± 0.02	+3.13	2.93 ± 0.24[d]	1	+0.21
A34	2.55 ± 0.62 and 4.86 ± 0.25[h]	1	+0.10 and −0.12	–	–	–	4.68 ± 0.07[f]	1	−0.30
E35	–	–	–	4.37 ± 0.03[b]	0.74 ± 0.03	+0.99	4.28 ± 0.15[b]	0.53 ± 0.08	+0.35
K36	–	–	–	4.60 ± 0.03[f]	1	−0.79	3.86 ± 0.20[b]	0.48 ± 0.08	+0.41
Q40	–	–	–	–	–	–	3.55 ± 0.03[f]	1	−0.67
Y41	–	–	–	–	–	–	4.29 ± 0.13[b]	0.62 ± 0.11	+0.30
A42	–	–	–	–	–	–	3.87 ± 0.05[f]	1	−0.43
N43	3.24 ± 0.40[f]	1	−0.14	–	–	–	3.99 ± 0.16[f]	1	+0.14[k]
D44	3.77 ± 0.07[f]	1	+0.35	3.65 ± 0.01[f]	1	+2.45	3.71 ± 0.02[l]	1	+1.48
V47	–	–	–	4.19 ± 0.04[f]	1	+0.51	4.06 ± 0.09[f]	1	+0.26
D48	4.00 ± 0.04[m]	0.87 ± 0.06	+0.65	4.03 ± 0.01[b]	0.74 ± 0.01	+3.01	3.92 ± 0.05[n]	1	+0.67
G49	2.76 ± 0.54 and 4.66 ± 0.15[h]	1	−0.11 and −0.24	–	–	–	2.93 ± 0.10[d]	1	+0.38
E50	2.70 ± 0.29[d]	1	−0.18	2.50 ± 0.29[b]	0.53 ± 0.07	−0.63	4.16 ± 0.05[m]	0.72 ±0.05	+0.66
W51	–	–	–	4.35 ± 0.09[m]	0.82 ± 0.04	+1.06	–	–	–
T52	–	–	–	4.65 ± 0.04[f]	1	−0.53	–	–	–
Y53	3.68 ± 0.46[m]	0.57 ± 0.25	−0.11	–	–	–	–	–	–

(Continued)

Table IV
(Coninued)

Residue	H^n Shift Change pK^{app}	H^n Shift Change Hill Coefficient	H^n Shift Change Magnitude[a] (ppm)	N^h Shift Change pK^{app}	N^h Shift Change Hill Coefficient	N^h Shift Change Magnitude (ppm)	C′ Shift Change pK^{app}	C′ Shift Change Hill Coefficient	C′ Shift Change Magnitude (ppm)
D54	–	–	–	3.47 ± 0.02[b]	0.89 ± 0.02	+2.18	3.80 ± 0.06[f]	1	+0.41
D55	3.07 ± 0.28[d]	1	−0.12	3.29 ± 0.02[b]	0.87 ± 0.02	+2.37	3.15 ± 0.04[b]	0.85 ± 0.04	+1.44
A56	3.68 ± 0.15[d]	1	+0.23	3.20 ± 0.02[f]	1	–1.57	3.28 ± 0.09[d]	1	+0.33
T57	3.62 ± 0.14[f]	1	+0.17	3.21 ± 0.06[b]	0.77 ± 0.05	+0.98	3.43 ± 0.15[b]	0.66 ± 0.10	–0.42
T59	3.04 ± 0.22[d]	1	+0.15	–	–	–	–	–	–
F60	4.57 ± 0.23[f]	1	+0.10	–	–	–	–	–	–
T61	–	–	–	–	–	–	3.91 ± 0.18[c]	0.59 ± 0.11	−0.29
V62	4.19 ± 0.14[f]	1	−0.15	3.57 ± 0.19 and 4.64 ± 0.12[j]	1	−0.51 and −0.72	3.37 ± 0.11[c]	0.71 ± 0.08	−0.52
T63	–	–	–	3.17 ± 0.09[b]	0.66 ± 0.06	+0.85	2.73 ± 0.05[f]	1	−0.67
E64	3.03 ± 0.12 and 4.55 ± 0.39[h]	1	−0.56 and −0.13	2.99 ± 0.01 and 4.55 ± 0.04[h]	1	+5.53 and +1.32	–	–	–

A fixed Hill coefficient value of 1 was used in each fit unless the fit was significantly better with a value different from 1.
[a]From low to high pH.
[b]The 1 pK_a plus Hill coefficient model was chosen. This was significant to $P < 0.01$.
[c]The 3 pK_as model was chosen. This was significant to $P < 0.01$. The additional pK_as are not shown as they are below the minimum shift change cut-off.
[d]The 2 pK_as model was chosen. This was significant to $P < 0.01$. The second pK_a is not shown as it is below the minimum shift change cut-off.
[e]The 3 pK_as model was chosen. This was significant to $P < 0.05$.
[f]The 1 pK_a model was chosen. No other model was significant to $P < 0.05$.
[g]The 1 pK_a plus Hill coefficient model was chosen. This was significant to $P < 0.05$.
[h]The 2 pK_as model was chosen. This was significant to $P < 0.01$.
[i]The 2 pK_as model was chosen. This was significant to $P < 0.05$.
[j]The 2 pK_as model was chosen. This was significant to $P < 0.025$.
[k]The total chemical shift change is below the cut-off value for consideration in this study but the chemical shift does show a small pH-dependent change affected by the titration of the D44 side chain.
[l]The 2 pK_as model was chosen. This was significant to $P < 0.05$. The second pK_a is not shown as it is below the minimum shift change cut-off.
[m]The 1 p*K*a plus Hill coefficient model was chosen. This was significant to $P < 0.025$.
[n]The 2 pK_as model was chosen. This was significant to $P < 0.025$. The second pK_a is not shown as it is below the minimum shift change cut-off.

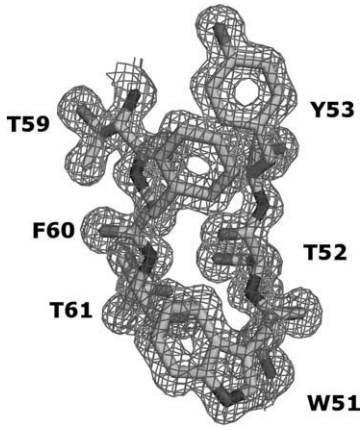

Figure 2

An example of the quality of the electron density for β-strands 3 and 4 of the 1.2 Å resolution pH 3.0 structure. Electron density from the 2|Fo-Fc| map is contoured at 1.0 sigma. This figure was produced using PyMOL.[41]

as shown in Figure 4(b). This conformation consists of the C-terminus occupying a similar position to that of the side chain in the high pH structures, whereas the side chain at pH 3.0 extends out into solution in the orientation in which the C-terminus is found at pH 4.0 and above, although the electron density around the side chain COOH group is weak at pH 3.0, suggesting disorder. In this conformation, the side chain is not able to form hydrogen bonds with K18 and D48, as it does at higher pH.

The loop between β-strands 1 and 2 (residues 17–19) also differs slightly in the pH 3.0 structure from the published structures, moving 0.7–0.9 Å closer to the centre of the protein compared with the 1pga structure, as shown in Figure 4(c), probably because of the movement of the E64 side chain out of this space. Other than this difference in loop position, no large changes in conformation are seen for K18, as expected from NMR data discussed later, which indicate the presence of different HSQC peaks at high and low pHs, suggesting a pH-dependent conformational change. However, the change in conformation observed for the E64 side chain results in the loss of a hydrogen bonding interaction involving the amide of K18, which could explain the major change observed in the K18 amide HSQC peak, particularly as K18 itself undergoes only a small conformational change between pH 3.0 and 4.0.

The NMR chemical shift data discussed later also show different peaks for D44 at high and low pHs, which suggests a conformational change for this residue. As discussed in a previous article,[20] this conformational change is also identified using relaxation dispersion data and is due to the loss of the final two residues of the α-helix upon protonation of the D44 side chain and the loss of the D44–Q40 side chain-side chain hydrogen bond, resulting in a shortening of the helix by two residues and some structural rearrangement of residues 43–47. This results in weak dimerisation at low pH. This structural change is not observed in the pH 3.0 crystal structure by comparison with the 1pga and 1pgb structures,[19] as shown in Figure 4(d). However, the two GB1 monomers in the asymmetric unit pack together *via* the last turn of the α-helix in both chains (residues Q40–N45). The D44 side chains of the two monomers approach close to each other in this packing, with 2.3 Å separating the carboxylate oxygens, which form a likely hydrogen bond (see inset of Fig. 3). As the crystals were formed at pH 5.5 and then soaked in a pH 3.0 buffer to effect a change in conformation to the pH 3.0 structure, D44 may have been prevented from undergoing a change in conformation, such as the solution data suggest, by these crystal packing contacts which could fix the residues in the conformation occupied at pH 5.5. The orientation of D44 may not, therefore, reflect that at pH 3.0 in solution, hence explaining the lack of a conformational change in this region in the pH 3.0 crystal structure.

Structural analysis of chemical shift changes

Our previous study[21] identified pK_a values for almost all of the titrating groups in GB1. In this study, we have identified a large number of pH-dependent chemical shift changes, and have been able to characterize them in

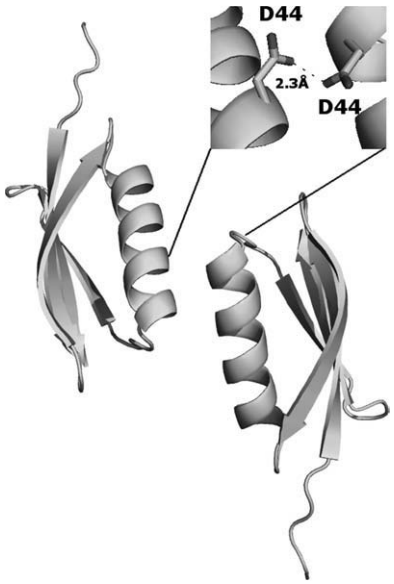

Figure 3

The packing of the two monomers of protein G within the asymmetric unit. The inset figure shows an expanded view of the final turns of the helices with the interaction between D44 side chains marked. This figure was produced using PyMOL.[41]

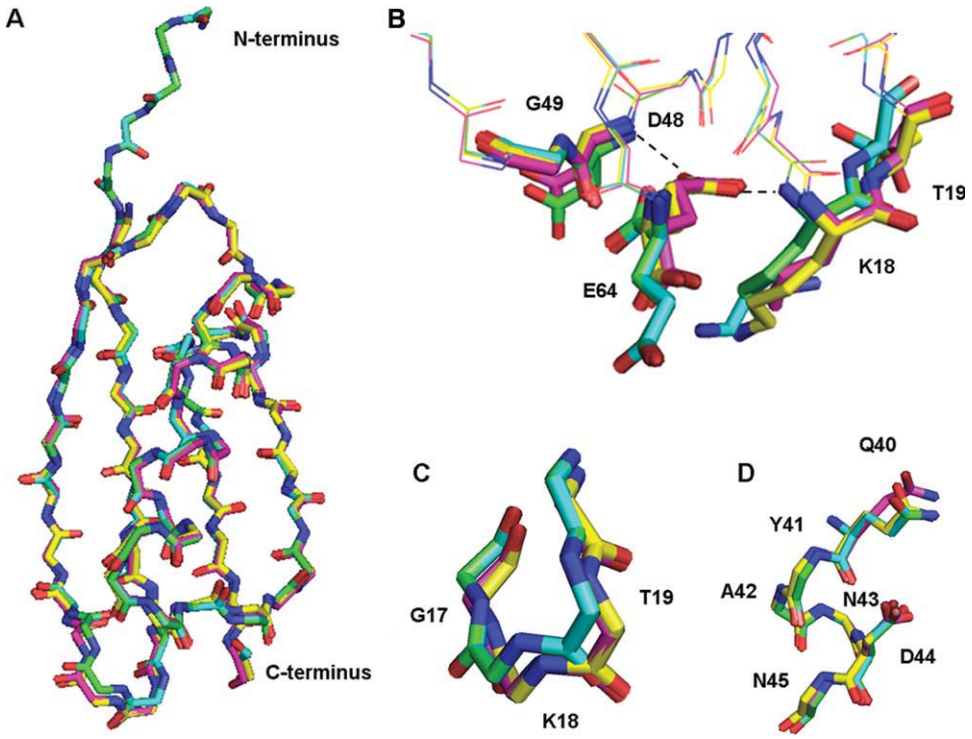

Figure 4

Overlays of the pH 3.0 structure with those determined by Gallagher *et al.*[19] Chain A of the pH 3.0 structure is shown in green, chain B of the pH 3.0 structure is shown in cyan, the 1pga structure is shown in yellow and the 1pgb structure is shown in pink.[19] The RMSD between the pH 3 and 1pga structures is 0.36 Å and the RMSD between the pH 3 and 1pgb structures is 0.30 Å. Chains were overlaid by minimization of the RMSD between aligned residues throughout the protein chain. Nitrogen atoms are shown in blue and oxygen atoms in red. This figure was produced using PyMOL.[41] (**A**) An overlay of the backbone of GB1 (side chains are omitted for clarity). (**B**) An enlargement of the C-terminal region showing the conformational change involving E64 and the loss of hydrogen bonds between the amides of K18 and D48 and the E64 side chain at pH 3.0. The residues with chemical shifts affected by the conformational change are shown as sticks while the main chain of the protein extending from this region is shown as lines. Hydrogen bonds to the E64 side chain at pH 4.0 and above are shown as dashed lines. (**C**) An enlargement of the β1-β2 loop viewed from within the protein, showing the movement of the loop at pH 3.0. (**D**) An enlargement of the C-terminal region of the α-helix, showing very little change in the structure between pH 4.5 and pH 3.0.

terms of pK^{app} values plus the associated high and low pH shifts. Comparison of the pK^{app} values measured here with the previously identified side chain pK_as allows a confident assignment of pH-dependent shift changes to specific side chain protonation events in most cases, supported by comparison of the pH 3.0 structure with the published pH 4.0 and 4.5 crystal structures.[19] In this section, we analyze the structural correlations that can be made.

Through-bond effects on chemical shifts

Titration of aspartate and glutamate side chains has a significant effect on the amide nitrogen and carbonyl carbon chemical shifts of the same residue, demonstrated by the observation that the shift changes have the same pK^{app} value as the side chain. The shift changes are 0.7–3.0 ppm in nitrogen shifts (excluding E64 which undergoes a conformational change and therefore has a larger shift change) and 0.3–1.5 ppm in carbon shifts, all of which are downfield shifts with increased pH, as previously observed for carbon shifts by Lindman *et al.*[42] and for nitrogen shifts by Betz *et al.*,[12] except for the nitrogen shift of E23 which moves upfield with increased pH. Large changes in the carbonyl carbon shifts of all aspartate and glutamate residues and the nitrogen chemical shifts of E23, E27, D30, E35, D44, D48, and E64 that fit to the pK_as of those residues' side chains[21,22] were observed, as shown in Figure 5, although D9, E50, and D54 do not show this effect on amide nitrogen shift. Similar changes are also observed in the carbonyl carbon shifts of residues preceding carboxylates and amide nitrogen shifts of residues following carboxylates in response to the titrating side chain, as shown by the carbonyl carbon shifts of M8, T26, V29, A34, and V47 (Fig. 6). N43 also shows a small change in carbonyl carbon shift that reflects the titration of D44 but this is below the cut-off imposed by this study. This change in chemical shift of the following or preceding residue is likely to be due to the nature of the amide bond, the change in chemical

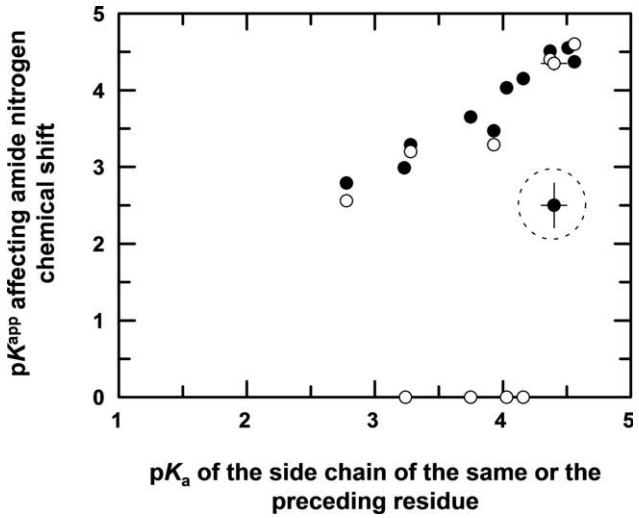

Figure 5

A comparison between the pK^{app}s affecting amide nitrogen chemical shifts and the pK_as of the side chains of the same or the preceding residues. Filled circles are the nitrogen shifts of carboxylate residues while open circles are the nitrogen shifts of residues following carboxylates. Circles on the *x* axis are titrating amino acids where the amide nitrogen of the amino acid following does not have a significant pH dependence. The ringed point shows that the nitrogen shift of E50 is affected by a low pH titration that does not match the pK_a of the side chain but is due to a chemical shift change in the C-terminal region of the β-sheet, discussed later in the context of cooperative effects. All residues had only one pK_a except for E64, where both pK_as were used, taking the pairs with closer values. Error bars are in most cases smaller than the circles.

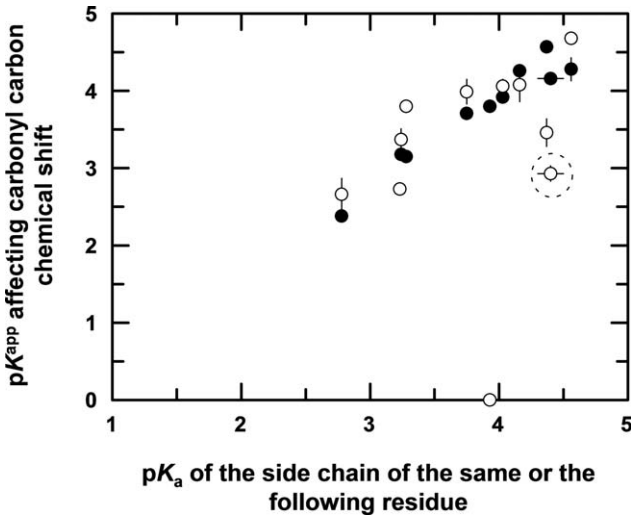

Figure 6

A comparison between the pK^{app}s affecting carbonyl carbon chemical shifts and the pK_as of the side chains of the same or following residues. The filled circles represent the carbonyl carbon shifts of carboxylate residues while the open circles represent the carbonyl carbon shifts of residues preceding carboxylates. The circle on the *x* axis is D54, for which Y53 C′ does not have a significant pH-dependent shift. The circled point is due to a chemical shift change in G49 at the C-terminal region of the β-sheet, discussed later in the context of cooperative effects. All residues had only one pK^{app}/pK_a except for E64, where the larger shift change was used. Error bars are in most cases smaller than the circles.

shift of one atom in that bond having a large influence on the other. Indeed, the chemical shifts of amide nitrogens and the preceding carbonyl carbon often share the same influence (Fig. 7), reflecting this relationship. Where the residue preceding a carboxylate is itself a carboxylate residue, however, this transmission is not observed in the carbonyl carbon shift, the effect of the titration of the side chain within the same residue being greater.

Through-space effects

The greatest pH-dependent effect on the amide proton chemical shift is through direct hydrogen bonding to carboxylate side chains. Four residues in GB1 form hydrogen bonds to carboxylates in the high pH crystal structure (K18, T33, D48, and A56 hydrogen bond to the side chains of E64, D30, E64, and D54 respectively, as shown in Fig. 8). The amide proton shifts of these residues show large upfield shifts in the range of 0.23–1.32 ppm with reduced pH. The magnitude of the change is related to the hydrogen bonding distance, with shorter hydrogen bonds causing a greater shift change as shown in Figure 9, although it is unclear how general this result is because the data are limited.

Bundi and Wüthrich[9] found that amide proton chemical shifts for residues that form hydrogen bonds to carboxylate side chains show marked changes with pH in

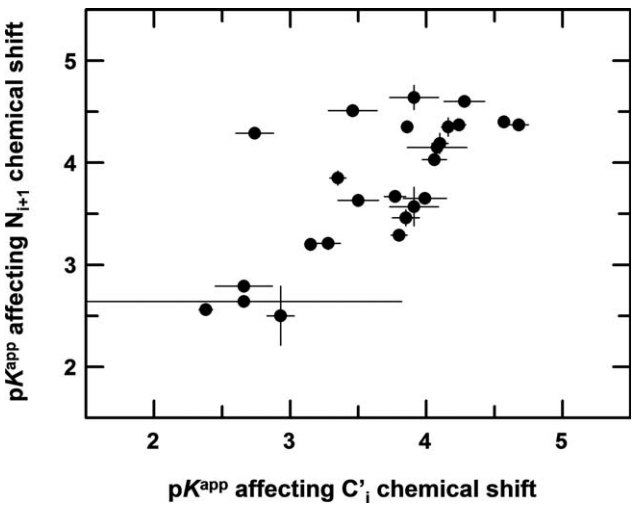

Figure 7

A comparison of the pK^{app} affecting the carbonyl carbon chemical shift of residue *i* with that affecting the amide nitrogen chemical shift of residue *i* + 1 for all cases in which a significant change in chemical shift is observed for both atoms. In cases where the chemical shift changes fit to multiple pK^{app}s, the larger magnitude shift was used unless both C′ and N had two pK^{app}s in which case both were used and the closer values were compared.

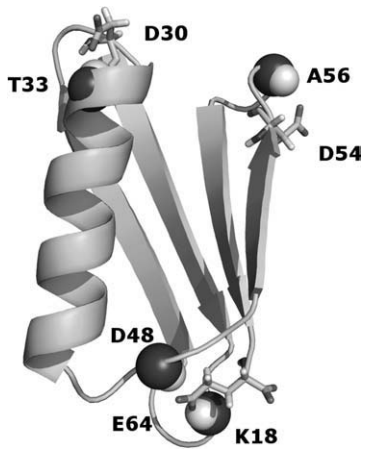

Figure 8

The amides that form hydrogen bonds to carboxylate side chains. This figure was produced using PyMOL[41] and the crystal structure of protein G determined by Gallagher *et al.*[19] (PDB ID: 1pga). Carboxylate side chains are shown as sticks. Amides forming hydrogen bonds to carboxylate side chains are shown as balls.

response to the titration of the carboxylate as the hydrogen bond becomes weaker, and therefore the bond length becomes greater, upon protonation of the carboxylate. This is due to the protonation making the carboxylate oxygen less electronegative. The large change in amide proton shift in response to the titration of hydrogen bonded carboxylate side chains has also been previously noted by Khare *et al.*[22]

The nitrogen shifts of these amides also show large changes in response to the titration of the hydrogen bonded carboxylate, as would be expected, but a similar dependence on the hydrogen bond length is not observed in the magnitude of these changes. In contrast to amide proton shifts nitrogen shifts show a greater dependence on through-bond effects than through-space effects, the chemical shift change of the amide nitrogen of D48 reflecting the titration of the D48 side chain rather than the hydrogen bonding to the E64 side chain. Likewise, the amide nitrogen shift of A56 is principally affected by the through-bond effect from D55 rather than the hydrogen bonding interaction with D54. However, the angle between the carboxylate oxygen and the N—C peptide bond for the D48–E64 hydrogen bond is 116° and that between the carboxylate oxygen of D54 and the C—N peptide bond for the D54–A56 hydrogen bond is 129° in the 1pga crystal structure. These angles are not particularly favorable for a large electrostatic effect from the side chain on the nitrogen shifts, possibly explaining the dominance of the through-bond effect observed in the pH-dependent shift changes.

Smaller but still large changes in proton shifts can also indicate the gain of a hydrogen bond interaction with carboxylic acid side chains at low pH, as seen for T57 and T10 due to changes in the positions of aspartate residues A56 and D9, respectively, in the pH 3.0 crystal structure that place them within hydrogen bonding distance of the amides.

In this context, it is worth noting that hydrogen bonding interactions can be observed directly by measurement of scalar couplings across the hydrogen bond. Such measurements have been made for protein G, and indicate that the four hydrogen bonds to carboxylates indicated in Figure 9 are present[43]; they do not however correlate well in magnitude with either the shift change or the hydrogen bond distance. Further studies on this topic are merited.

Through-space effects from His tag

Several residues show small changes in amide proton and nitrogen and carbonyl carbon chemical shifts that reflect titrations with pK^{app}s in the range 5.0–7.0. These pK^{app}s are too high to be related to the titration of carboxylate side chains but are in the range in which histidines titrate. The only histidines present in the protein are within the N-terminal histidine tag (MH_6AMD), suggesting these residues interact with the histidine tag in solution. The affected residues are found in the region of the protein close to the N-terminus (the affected shifts being the amide protons of D9, E27, V29, D55, and A56, the amide nitrogens of T33 and K58 and the carbonyl carbons of M8, D9, T10, and A56), as shown in Figure 10 and Table V. Most of these changes are below the cut-off values applied during this study, the exceptions being the amide proton and carbonyl carbon shifts of A7 and the amide nitrogen shift of M8, both residues from the N-terminal tag rather than the native protein sequence.

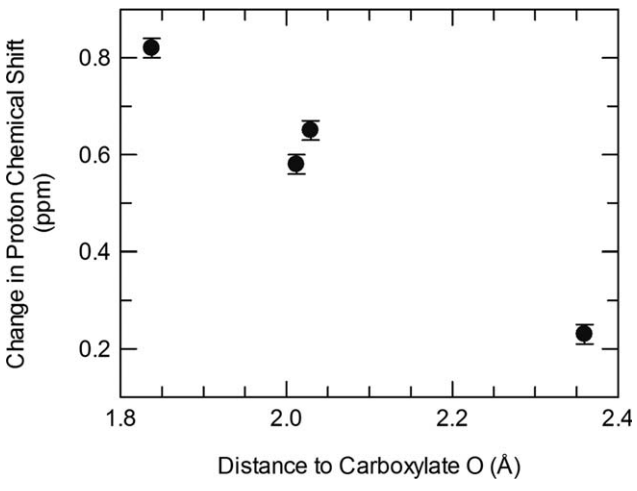

Figure 9

The relationship between the amide proton shift change and the distance to the carboxylate O atom for amides forming hydrogen bonds to carboxylate side chains.

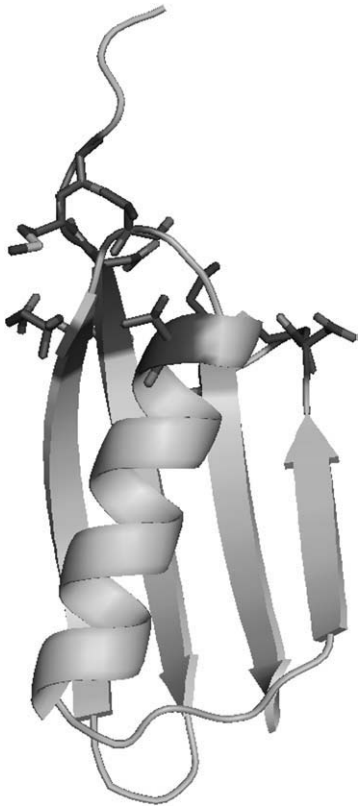

Figure 10

The pH 3.0 structure of protein G with those residues that show pH-dependent changes in amide nitrogen or proton or carbonyl carbon chemical shifts that fit to pK^{app}s expected to relate to the titration of histidine residues within the tag shaded black with side chains shown as sticks. These residues cluster in the region of the protein close to the histidine tag. This figure was produced using PyMOL.[41]

The nature of the interaction between these residues and the histidines in the tag cannot be determined as in the pH 3.0 structure only the last three histidines of the tag can be observed but the electron density is weak for these residues, indicating disorder, and the remaining three histidines are not visible, whereas there is no tag in the other crystal structures. Given the disorder apparent from the crystal structure and the small change in chemical shift, it is likely that these interactions are transient, possibly explaining the low magnitude of the changes. However, significantly it is clear that tag residues do interact with residues from the native protein sequence and can therefore complicate analysis of chemical shift changes if the tag is not removed after purification.

Comparison of the results reported in this section with those reported in the previous section suggests that the chemical shift effect of the weak and transient hydrogen bonds formed to the histidines is between 5 and 20 times less than that from the almost 100% populated hydrogen bonds to carboxylates. Interestingly, this provides some indication of the aggregate population of the hydrogen bonds to histidines, that is, that hydrogen bonds are likely to be present ~10% of the time.

Conformation-dependent effects

Comparison of the pH 3.0 crystal structure to the previously published structures[19] identified a pH-dependent conformational change in the C-terminal E64 residue, as discussed previously. Large changes in amide proton chemical shifts reflecting this conformational change are also observed in the β1-β2 loop (K18–L20) and the loop linking the C-terminus of the α-helix with β-strand 3 (D48–G49) that flank the E64 residue [Fig. 4(b)]. Changes in hydrogen bonding directly cannot explain the effects on T19, L20, and G49; however, as these residues do not form hydrogen bonds to E64 in either the pH 3.0 or the higher pH crystal structures as the distances visible in the pH 4.5 and 4.0 crystal structures are too long for hydrogen bonding to T19, and the G49 amide extends from the opposite side of the protein chain from E64 and so cannot hydrogen bond to it. In addition, the conformation of E64 at pH 3.0 makes hydrogen bonding between E64 and the amides of T19 and G49 even less likely. Therefore, the large change in amide chemical shifts for these residues is likely to be due to the change in conformation in this region. The chemical shift changes for the amides of T19 and G49 are smaller than those of K18 and D48, implying that the conformational change has less effect on amide proton shifts than direct hydrogen bonding to the E64 side chain.

The nitrogen chemical shifts of G17 and L20 both show pH-dependent changes that fit to the pK_a of the E64 side chain, providing further evidence that the pH-dependent conformational change in E64 induces a change in the loop G17–L20.

As discussed in an earlier publication[20] based on both chemical shift and relaxation dispersion information, the C-terminal turn of the α-helix undergoes a conformational change in response to the protonation of D44 and the

Table V

The Small Changes in Chemical Shifts due to the Titration of Histidine Residues in the Tag

Residue	Atom Undergoing a pH-Dependent Shift Change	pK^{app} Influencing the Change in Shift	Magnitude of the Change in Shift from Low to High pH (ppm)
M8	C′	6.58 ± 0.19	+0.16
D9	H_N	5.14 ± 0.55	−0.04
D9	C′	6.25 ± 0.16	+0.19
T10	C′	6.20 ± 0.51	+0.07
E27	H_N	5.55 ± 0.37	−0.06
V29	H_N	5.72 ± 1.57	−0.02
T33	N_H	5.99 ± 0.19	+0.14
D55	H_N	6.20 ± 1.41	−0.02
A56	H_N	5.64 ± 1.24	−0.03
A56	C′	7.16 ± 1.00	−0.03
K58	N_H	5.11 ± 0.45	+0.23

consequent loss of the D44–Q40 side chain-side chain hydrogen bond. Although not observed in the pH 3.0 crystal structure because of crystal packing contacts, evidence of this conformational change is seen in the pH-dependent chemical shift changes. The side chain N_ϵ and $H_{\epsilon 1}$ chemical shifts of Q40 both undergo large pH-dependent changes that fit to the pK_a of D44, indicating a hydrogen bond between the two side chains that is lost upon protonation of D44. Such a hydrogen bond is visible in approximately half of the published crystal structures of GB1. The amide proton and nitrogen shifts of D44 also show a large pH-dependent change fitting to the pK_a of D44. The change in proton as well as nitrogen shifts in this case indicate that the change is not a through-bond effect with no conformational change as no other proton shifts of residues that have no conformational change show such an effect in GB1. Also affected are Q40 C′ (shift change −0.67 ppm, pK^{app} 3.55 ± 0.03), A42 C′ (shift change −0.43 ppm, pK^{app} 3.87 ± 0.05), N43 NH (shift change −0.14 ppm, pK^{app} 3.24 ± 0.40), N43 Nδ (shift change −0.59 ppm, pK^{app} 3.70 ± 0.03) and D44 C′ (shift change + 1.48 ppm, pK^{app} 3.71 ± 0.02). Of these, the changes in D44 N and C′ shifts are most likely a through-bond effect from their own side chain. However, the others clearly reflect a pH-dependent event related to the protonation of D44 and weakening of the hydrogen bond to Q40. The very large chemical shift changes of D44 H and N and of Q40 C′ strongly indicate that the hydrogen bond between D44 HN and Q40 O is broken at lower pH: both the sign and the magnitude of the shift changes are consistent with hydrogen bonding as the origin of the change.[44,45]

The large conformation-dependent changes in chemical shifts are often of a similar magnitude to the through-space effects caused by direct hydrogen bonding to titrating side chains. Importantly, this indicates that care must be taken when analyzing such data as the different effects cannot be distinguished on the basis of magnitude.

Cooperative effects

The effects described above account for most of the nuclei that have significant pH-dependent chemical shift changes. Most of the remaining pH-dependent changes can be accounted for by two interesting cooperative effects.

The amide proton and nitrogen and the carbonyl carbon chemical shifts of residues 30–33 (excluding the amide nitrogen shift of A32) in the N-terminus of the α-helix all show small changes in response to the titration of the D30 side chain. The amides of these residues, with the exception of T33, are unlikely to form hydrogen bonds to the side chain of D30. D30, however, forms an α-helix cap in the crystal structure, forming a hydrogen bond to the amide of T33 to stabilize the N-terminus of the α-helix. Such capping interactions are well documented.[46,47] Protonation of the D30 side chain would be expected to weaken this hydrogen bond, possibly causing the N-terminus of the helix to become less stable. The change in chemical shift of these first α-helix residues, therefore, is likely to reflect a slight "fraying" of the N-terminus of the α-helix upon protonation of this capping residue as the N-terminus of the helix becomes less stable. "Fraying" of the helix upon protonation of the capping D30 side chain would be expected to affect the chemical shifts of all three atoms as the structure of the N-terminus of the helix would be altered. Therefore, the identification of the same effect upon amide proton, nitrogen and carbonyl carbon chemical shifts suggests that the weakening of the D30 carboxylate-T33 amide hydrogen bond by protonation of the D30 side chain causes some disturbance in the structure of the first turn of the α-helix at low pH. This helix "fraying" is not visible in the pH 3.0 crystal structure because this is above the pK_a of D30 and so the side chain is >50% deprotonated at pH 3.0. It is therefore not unreasonable that it should remain hydrogen bonded to the amide of T33 in the crystal structure, as at pH 4.5.

An α-helix is thought to be a cooperative unit, alterations in one part of the helix affecting the whole structure. However, these data suggest that the effect on the N-terminus of the helix upon protonation of the D30 side chain is not propagated further than the first turn, the remainder of the helix structure being completely unaffected as suggested by the lack of pH-dependent chemical shift changes. This implies that the hydrogen bond network in an α-helix does not necessarily function as a completely cooperative unit, and indeed in this case there seems to be a break in the cooperativity at T33, because residues beyond here show very little effect.

Another example of chemical shift changes in a cooperative network is seen in the β-sheet. The carbonyl carbon shift of G49, the amide proton and nitrogen shifts of E50 and the carbonyl carbon shift of T63 show pH-dependent changes that fit to a pK^{app} of 2.7 ± 0.2 (Fig. 11). These changes in E50 and G49 chemical shifts are those ringed in Figures 5 and 6 above. These residues are clustered in the β-sheet near the C-terminus of GB1, the amide of E50 forming a hydrogen bond with the carbonyl of T63. The cause of this chemical shift change is not known as the only residue that titrates with a pK_a close to 2.7 is D30, in the N-terminus of the α-helix but this is too far from the affected residues in the crystal structure to be likely to affect them, particularly without causing any effect on the intervening residues. However, the close similarity of the pK^{app} of all these residues strongly suggests a common origin of the effect.

There is also a second cluster of residues adjacent to this with a pK^{app} of 3.8 ± 0.2, comprising the amide proton of L15, amide nitrogen and proton and carbonyl carbon of N16, amide nitrogen and proton of K21, carbonyl carbon of T61, and amide nitrogen and proton of V62 (Fig. 11). Although the pK^{app}s of these residues are slightly variable, their close proximity and similar pK^{app}s suggests again a common origin. Thus approximately one-third of the residues within the four-stranded sheet form two contiguous

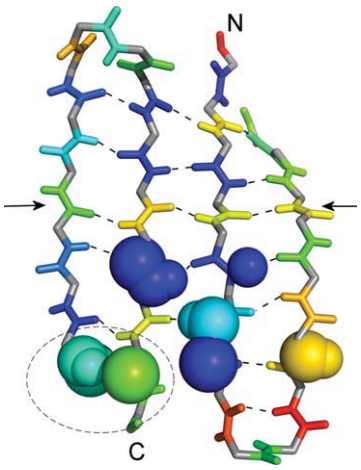

Figure 11

The β-sheet region of GB1. Cross-strand hydrogen bonds are indicated by dashed lines. Nuclei showing otherwise unexplained pH-dependent chemical shift changes with a pK^{app} of 3.8 ± 0.2 are indicated by spheres; those titrating with a pK^{app} of 2.8 ± 0.2 are also indicated by spheres within the dashed region close to the C-terminus. These residues each form a contiguous unit, which is suggested to indicate the presence of a cooperative pH-dependent change. For comparison, the colors on backbone amide units denote the magnitude of the oscillation in amide plane (γ-GAF) determined by Bouvignies *et al.*,[48] ranging from zero (blue) through green, yellow and orange to ~30° (red). The two arrows indicate the dynamic barrier discussed in the text.

cooperative networks in which the pH-dependent conformational change is propagated throughout the network.

DISCUSSION

GB1 is a small and rather simple protein domain, which makes it a useful model with which to study the relationship between structural changes and pH-dependent chemical shifts. Unlike the proteins used in previous studies,[12] GB1 is not an enzyme and has no unusual pK_as or complex hydrogen bond networks, making the analysis of chemical shift data simpler.

Through-bond effects

The titration of an aspartate or glutamate side chain affects the chemical shifts of both the amide nitrogen and carbonyl carbon in the amide groups on both sides of it. Because the chemical shift is an indicator of the electron density and distribution around a nucleus, this reinforces the point that a backbone amide group is a single π-electron system. It also shows that significant changes to electron density can be passed on through up to six chemical bonds.

The titration of an aspartate or glutamate residue had effects of <0.1 ppm on the amide proton shift of that residue, consistent with the size of intrinsic titration shifts observed by Bundi and Wüthrich.[9] The two exceptions are the C-terminal glutamate and D44, where in both cases the larger shift changes are due to conformational change.

The pH-dependent changes in amide proton chemical shifts in the B1 domain of protein G have been previously studied by Khare *et al.*[22] They observed large changes in amide proton shift for K18, T33, and D48, all of which are involved in hydrogen bonds to carboxylate side chains in the crystal structure,[22] in agreement with the results of this study. A smaller pH-dependent change in proton chemical shift was observed for T19 which was explained as due to its proximity to the K18–E64 hydrogen bond. In light of the crystal structure of GB1 at pH 3.0, however, we suggest that this pH-dependent change in shift is due to the effects of the structural rearrangement of the E64 residue with reduced pH. In addition, the H_ϵ proton chemical shift of Q40 was found to titrate with a pH midpoint that corresponds to the pK_a of the D44 side chain to which the side chain of Q40 forms a hydrogen bond in the crystal structure,[22] an effect also observed in this study and discussed in relation to a structural change in the C-terminus of the helix in a previous publication.[20] The Khare *et al.*[22] study, however, did not have a low pH structure available to compare changes directly to observed changes in structure.

Changes in carbonyl chemical shifts with pH have also been studied for a limited number of residues in a mutant of GB1.[42] Carbonyl chemical shift changes with pH were studied for 28 of the 56 residues, 21 of these showing pH-dependent changes in chemical shift.[42] Backbone carbonyls of aspartate and glutamate residues showed large shift changes on titration of the carboxylate, in agreement with the present study. Some residues that precede or follow a carboxylate in the protein sequence were also shown to exhibit a pH-dependent change in chemical shift reporting the pK_a of the neighboring carboxylate.[42] Lindman *et al.*[42] suggested that the effect of the titration of acidic side chains on carbonyls separated from the side chain by a small number of covalent bonds, such as the carboxyl of the same residue, is due to a through-bond effect. This is supported by this study which found similar effects for both nitrogen and carbonyl carbon shifts of titrating residues, but not the amide proton shifts. In summary, although through-bond effects on ^{13}C and ^{15}N shifts are reasonably predictable and occur over up to six bonds, local effects can sometimes cause unusual titration behavior.

Through-space effects

Amide proton and nitrogen shifts for the same amide group are expected to be influenced predominantly by the same effects as both are expected to be influenced significantly by hydrogen bonding. However, it is apparent that many residues show effects on amide proton but not nitrogen shifts or vice versa, suggesting a significant influence of differing effects. Upon closer inspection, however, those residues that show changes in both amide nitrogen and proton shifts do report the influence of the same pK^{app} as shown in Figure 12, but do not show a correlation in the

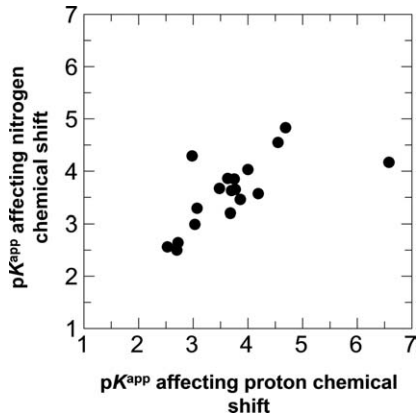

Figure 12

A comparison of the pK^{app} affecting the amide proton chemical shift with that affecting the amide nitrogen shift of the same residue. Only those residues for which both the proton and nitrogen shifts undergo pH-dependent changes are shown.

magnitude of the change. The difference in the response of the amide nitrogen and proton shifts to the titration of carboxylate residues can be explained by the geometry of the through-space interaction with the carboxylate side chain. One would expect carboxylates to affect the chemical shift of H-bonded HN by an electric field effect[2,49]: the negative charge pushes electron density away from the proton down the HN bond. The magnitude of the chemical shift change is therefore proportional to cosθ, where θ is the angle between the CO_2^-—H and H—N vectors. The chemical shift change of N is also produced by an electric field effect, but in this case it depends on the angle between the CO_2^-—N and N—C′ vectors, which is of course a completely different geometry. Therefore, the interaction of an amide with a titrating side chain can have effects of differing magnitude on the amide proton and nitrogen because of the different relative orientations of these two bonds to the titrating side chain, explaining the differing effects on amide proton and nitrogen shifts observed in this study. A greater understanding of such effects is clearly important. First, because when studying chemical shift changes, for example by chemical shift mapping/chemically induced shifts, the amide proton and nitrogen shifts changes are often combined.[50,51] This difference in the magnitude of the effect however, suggests more information may be obtained if the proton and nitrogen shifts were analyzed separately. Second, because improved calculations of through-space titration effects allow other effects, such as pH-induced conformational change, to be more clearly identified.[52]

Conformational effects

Large changes in amide proton chemical shifts in response to conformational changes in GB1 were observed in the C-terminal region of the protein and in the last turn of the α-helix, particularly in D44. In the case of E64, such changes are observed in the amide proton shifts of residues surrounding the conformational change but without a direct hydrogen bonding interaction with E64. A similar effect is not seen in the amide nitrogen shifts of these residues This suggests that through-space effects due to the conformational change have a greater influence on the amide proton shift than on the amide nitrogen, although this could be a consequence of the different angles between the charged side chain and the polarisable bond. This does, however, indicate that large pH-dependent changes in amide proton shifts (of up to 0.5 ppm) do not necessarily indicate residues that form direct hydrogen bonds with titrating side chains.

Cooperative effects

pH-dependent chemical shifts are potentially well suited to the study of cooperative effects propagated throughout hydrogen bond networks because the transmission of effects can be followed by comparison of the pK^{app}s affecting chemical shift changes. Such transmission of shifts through a hydrogen bonding network has been described previously.[53,54] Parker *et al.*[53] found that hydrogen bonding to the carbonyl of the same residue as the amide of interest (secondary hydrogen bonding) and hydrogen bonding that does not directly involve the amide of interest but that forms a network around it can affect the amide proton chemical shift. This "cooperative" hydrogen bonding can have effects on the amide proton chemical shift of up to 1.3 ppm (secondary hydrogen bonding) or 1.1 ppm (tertiary hydrogen bonding).[53] They found that the key determinants of the chemical shifts of amide protons involved in hydrogen bonds are a through-bond effect caused by the primary hydrogen bond and the nature and number of secondary and tertiary hydrogen bonding partners.[53] The chemical shifts of amide protons that form hydrogen bonds with charged side chains, however, could not be predicted as accurately as amides involved in main chain-main chain hydrogen bonds.[53] Because of the fact that hydrogen bonding has major effects on amide proton shifts, one interpretation of this observation is that cooperative networks alter the strength of the hydrogen bonds; the direction of the effect noted by Parker *et al.*[53] suggesting that hydrogen bonds within a network are stronger than isolated hydrogen bonds.

Studies of amide chemical shift changes in adipocyte lipid-binding protein upon binding to *R*- and *S*-ibuprofen[54] showed changes throughout the backbone that occur in a regular pattern and seem to indicate that the chemical shift changes are passed on from β-strand to β-strand, propagating throughout the β-sheet. This suggested a concerted change in the hydrogen bond network in the protein to accommodate ligand binding.[54]

The correlated change in amide proton, nitrogen and carbonyl carbon chemical shifts in the first turn of the

α-helix indicate a fraying of the α-helix in response to the protonation of D30. The limiting of this effect to the first turn of the helix, however, indicates that the α-helix is not a single cooperative unit. Instead there appears to be a break in the cooperativity of the helix at T33, residues beyond this showing no effects of this fraying.

A very interesting set of correlated shift changes occurs at one end of the β-sheet, and involves three of the four strands (Fig. 11). The pK^{app} of 3.8 ± 0.2 does not correspond to any single neighboring residue, and may therefore reflect a cooperative structural change involving more than one titratable group. There is an interesting relationship between these residues and the backbone oscillations described by Bouvignies *et al.*[48] These authors used NMR measurements to characterize oscillations of the amide plane, described by a Gaussian axial fluctuation (GAF). They describe slow-timescale correlated motions across β-strands, which form a "standing wave" across the sheet. A particularly noticeable one involves the set of four amides marked by arrows in Figure 11, forming a line of fluctuating hydrogen bonds across the sheet. The interesting relationship is that these four amides appear to form a natural barrier to the correlated pH-dependent shift change seen here: in other words, the boundary of the correlated unit is dictated by slow motional fluctuations, which place a limit on correlated hydrogen bonding. Bouvignies *et al.*[48] suggest that the regions of the protein with restricted motion (the blue/green regions of Figure 11, which include the residues found here to have a correlated pH-dependent change) are motionally restricted because their large hydrophobic side chains tether them together. In other words, their data imply that correlated hydrogen bonding units are most stable within the hydrophobic core. This matches nicely with the expected lower dielectric constant in such regions, which may be expected to strengthen hydrogen bonding interactions. We have therefore labeled this region an "iceberg": the name recalls the standard model of liquid water, which consists of regions of ice-like regular hydrogen bonds, bounded by disordered regions. The icebergs are stabilized by the enthalpy of formation of hydrogen bonds, while the disordered regions have less favorable hydrogen bonds but have more favorable entropy. We suggest that the same balance occurs within the interior of the protein, with the interesting difference that the iceberg regions are stabilized by the hydrophobic core.

In summary, a detailed analysis of pH-dependent chemical shift changes in GB1 has found that almost all chemical shift changes can be understood on the basis of the change in structure with pH. They demonstrate that the protein undergoes a range of structural and dynamic changes, some of which are limited to the immediate vicinity of titrating groups and others of which are transmitted further, even across several strands of the β-sheet. The result gives an insight into the complexity and subtlety of protein structure and dynamics.

ACKNOWLEDGMENTS

The authors thank the Biotechnology and Biological Sciences Research Council for studentships (to JHT and VLG), and Diamond IO2 beamline staff for station alignment and helping with data collection.

REFERENCES

1. Neal S, Nip AM, Zhang H, Wishart DS. Rapid and accurate calculation of protein ^{1}H, ^{13}C and ^{15}N chemical shifts. J Biomol NMR 2003;26:215–240.
2. Williamson MP, Asakura T. Empirical comparisons of models for chemical-shift calculation in proteins. J Magn Reson B 1993; 101:63–71.
3. Montalvao RW, Cavalli A, Salvatella X, Blundell TL, Vendruscolo M. Structure determination of protein-protein complexes using NMR chemical shifts: case of an endonuclease colicin-immunity protein complex. J Am Chem Soc 2008;130:15990–15996.
4. Cavalli A, Salvatella X, Dobson CM, Vendruscolo M. Protein structure determination from NMR chemical shifts. Proc Natl Acad Sci USA 2007;104:9615–9620.
5. Shen Y, Lange OF, Delaglio F, Rossi P, Aramini JM, Lui G, Eletsky A, Wu Y, Singarapu KK, Lemak A, Ignatchenko A, Arrowsmith CH, Szyperski T, Montelione GT, Baker D, Bax A. Consistent blind protein structure generation from NMR chemical shift data. Proc Natl Acad Sci USA 2008;105:4685–4690.
6. Wishart DS, Arndt D, Berjanskii M, Tang P, Zhou J, Lin G. CS23D: a web server for rapid protein structure generation using NMR chemical shifts and sequence data. Nucleic Acids Res 2008; 36:W496–W502.
7. Wilton DJ, Kitahara R, Akasaka K, Williamson MP. Pressure-dependent ^{13}C chemical shifts in proteins: origins and applications. J Biomol NMR 2009;44:25–33.
8. Wilton DJ, Tunnicliffe RB, Kamatari YO, Akasaka K, Williamson MP. Pressure-induced changes in the solution structure of the GB1 domain of protein G. Proteins 2008;71:1432–1440.
9. Bundi A, Wüthrich K. Use of amide ^{1}H-NMR titration shifts for studies of polypeptide conformation. Biopolymers 1979;18:299–311.
10. Ebina S, Wüthrich K. Amide proton titration shifts in bull seminal inhibitor IIA by two-dimensional correlated ^{1}H nuclear magnetic resonance (COSY). Manifestation of conformational equilibria involving carboxylate groups. J Mol Biol 1984;179:283–288.
11. Clark AT, Smith K, Muhandiram R, Edmondson SP, Shriver JW. Carboxyl pK_a values, ion pairs, hydrogen bonding, and the pH-dependence of folding in the hyperthermophile proteins Sac7d and Sso7d. J Mol Biol 2007;372:992–1008.
12. Betz M, Löhr F, Weink H, Rüterjans H. Long-range nature of the interactions between titratable groups in *Bacillus agaradhaerens* family 11 xylanase: pH titration of *B. agaradhaerens* xylanase. Biochemistry 2004;43:5820–5831.
13. Haruyama H, Qian Y-Q, Wüthrich K. Static and transient hydrogen-bonding interactions in recombinant desulfatohirudin studied by ^{1}H nuclear magnetic resonance measurements of amide proton exchange rates and pH-dependent chemical shifts. Biochemistry 1989;28:4312–4317.
14. Schaller W, Robertson AD. pH, ionic strength and temperature dependence of ionization equilibria for the carboxyl groups in turkey ovomucoid third domain. Biochemistry 1995;34: 4714–4723.
15. Quirt AR, Lyyerla JR, Jr, Peat IR, Cohen JS, Reynolds WF, Freedman MH. Carbon-13 nuclear magnetic resonance titration shifts in amino acids. J Am Chem Soc 1974;96:570–574.
16. Surprenant HL, Sarneski JE, Key RR, Byrd JT, Reilley CN. Carbon-13 NMR studies of amino acids: chemical shifts, protonation shifts, microscopic protonation behavior. J Magn Reson 1980;40:231–243.

17. Rabenstein DL, Sayer TL. Carbon-13 chemical shift parameters for amines, carboxylic acids, and amino acids. J Magn Reson 1976;24:27–39.
18. Batchelor JG, Feeney J, Roberts GCK. Carbon-13 NMR protonation shifts of amines, carboxylic acids and amino acids. J Magn Reson 1975;20:19–38.
19. Gallagher T, Alexander P, Bryan P, Gilliland GL. Two crystal structures of the B1 immunoglobulin-binding domain of *Streptococcal* Protein G and comparison with NMR. Biochemistry 1994; 33:4721–4729.
20. Tomlinson JH, Craven CJ, Williamson MP, Pandya MJ. Dimerization of protein G B1 domain at low pH: a conformational switch caused by loss of a single hydrogen bond. Proteins 2010; 78:1652–1661.
21. Tomlinson JH, Ullah S, Hansen PE, Williamson MP. Characterisation of salt bridges to lysines in the Protein G B1 domain. J Am Chem Soc 2009;131:4674–4684.
22. Khare D, Alexander P, Antosiewicz J, Bryan P, Gilson M, Orban J. pK_a measurements from nuclear magnetic resonance for the B1 and B2 immunoglobulin G-binding domains of protein G: comparison with calculated values for nuclear magnetic resonance and x-ray structures. Biochemistry 1997;36:3580–3589.
23. Tunnicliffe RB, Waby JL, Williams RJ, Williamson MP. An experimental investigation of conformational fluctuations in proteins G and L. Structure 2005;13:1677–1684.
24. Joshi MD, Sidhu G, Nielsen JE, Brayer GD, Withers SG, McIntosh LP. Dissecting the electrostatic interactions and pH-dependent activity of a family 11 glycosidase. Biochemistry 2001;40: 10115–10139.
25. Sundd M, Iverson N, Ibarra-Molero B, Sanchez-Ruiz JM, Robertson AD. Electrostatic interactions in ubiquitin: stabilization of carboxylates by lysine amino groups. Biochemistry 2002;41:7586–7596.
26. Crennell SJ, Cook D, Minns A, Svergun D, Andersen RL, Nordberg-Karlsson E. Dimerisation and increase in active site aromatic groups as adaptations to high temperatures: x-ray solution scattering and substrate-bound crystal structures of *Rhodothermus marinus* endoglucanase. J Mol Biol 2006;356:57–71.
27. Krengel U, Dey R, Sasso S, Ökvist M, Ramakrishnan C, Kast P. Preliminary x-ray crystallographic analysis of the secreted chorismate mutase from *Mycobacterium tuberculosis*: a tricky crystallization problem solved. Acta Crystallogr Sect F Struct Biol Cryst Commun 2006;62:441–445.
28. Leslie AGW. Recent changes to the MOSFLM package for processing film and image plate data. Joint CCP4 and ESF-EAMCB Newslett Protein Crystallogr 1992;26.
29. CCP4. The CCP4 suite: programs for protein crystallography. Acta Crystallogr D Biol Crystallogr 1994;50:760–763.
30. Evans PR. Scaling and assessment of data quality. Acta Crystallogr D Biol Crystallogr 2005;2:72–82.
31. Navaza J. AMoRe: an automated package for molecular replacement. Acta Crystallogr A 1994;50:157–163.
32. Murshudov GN, Vagin AA, Dodson EJ. Refinement of macromolecular structures by the maximum-likelihood method. Acta Crystallogr D Biol Crystallogr 1997;53:240–255.
33. Emsley P, Cowtan K. Coot: model-building tools for molecular graphics. Acta Crystallogr D Biol Crystallogr 2004;60:2126–2132.
34. Gronenborn AM, Filpula DR, Essig NZ, Achari A, Whitlow M, Wingfield PT, Clore GM. A novel, highly stable fold of the immunoglobulin binding domain of *Streptococcal* Protein G. Science 1991; 253:657–661.
35. Strop P, Marinescu AM, Mayo SL. Structure of a protein G helix variant suggests the importance of helix propensity and helix dipole interactions in protein design. Protein Sci 2000;9:1391–1394.
36. Frericks Schmidt HL, Sperling LJ, Gao YG, Wylie BJ, Boettcher JM, Wilson SR, Reinstra CM. Crystal polymorphism of protein GB1 examined by solid-state NMR spectroscopy and X-ray diffraction. J Phys Chem B 2007;111:14362–14369.
37. Nauli S, Kuhlman B, Le Trong I, Stenkamp RE, Teller DC, Baker D. Crystal structures and increased stabilization of the protein G variants with switched folding pathways NuG1 and NuG2. Protein Sci 2002;11:2924–2931.
38. Wunderlich M, Max KE, Roske Y, Mueller U, Heinemann U, Schmid FX. Optimization of the gbeta1 domain by computational design and by in vitro evolution: structural and energetic basis of stabilization. J Mol Biol 2007;373:775–784.
39. Frank MK, Dyda F, Dobrodumov A, Gronenborn AM. Core mutations switch monomeric protein GB1 into an intertwined tetramer. Nat Struct Biol 2002;9:877–885.
40. Seewald MJ, Pichumani K, Stowell C, Tibbals BV, Regan L, Stone MJ. The role of backbone conformational heat capacity in protein stability: temperature dependent dynamics of the B1 domain of *Streptococcal* protein G. Protein Sci 2000;9:1177–1193.
41. DeLano WL. The PyMOL molecular graphics system. Palo Alto, CA, USA: DeLano Scientific; 2002.
42. Lindman S, Linse S, Mulder FAA, André I. pK_a values for side-chain carboxyl groups of a PGB1 variant explain salt and pH-dependent stability. Biophys J 2007;92:257–266.
43. Cornilescu G, Ramirez BE, Frank MK, Clore GM, Gronenborn AM, Bax A. Correlation between $^{3h}J_{NC'}$ and hydrogen bond length in proteins. J Am Chem Soc 1999;121;6275–6279.
44. Xu XP, Case DA. Probing multiple effects on ^{15}N, $^{13}C\alpha$, $^{13}C\beta$, and $^{13}C'$ chemical shifts in peptides using density functional theory. Biopolymers 2002;65:408–423.
45. Asakura T, Taoka K, Demura M, Williamson MP. The relationship between amide proton chemical shifts and secondary structure in proteins. J Biomol NMR 1995;6:227–236.
46. Penel S, Hughes E, Doig AJ. Side-chain structures in the first turn of the α-helix. J Mol Biol 1999;287:127–143.
47. Doig AJ, Baldwin RL. N- and C-capping preferences for all 20 amino acids in α-helical peptides. Protein Sci 1995;4:1325–1336.
48. Bouvignies G, Bernardó P, Meier S, Cho K, Grzesiek S, Brüschweiler R, Blackledge M. Identification of slow correlated motions in proteins using residual dipolar and hydrogen-bond scalar couplings. Proc Natl Acad Sci USA 2005;102:13885–13890.
49. Hass MA, Jensen RM, Led JJ. Probing electric fields in proteins in solution by NMR spectroscopy. Proteins 2008;72:333–343.
50. Deakin JA, Blaum B, Gallagher JT, Uhrin D, Lyon M. The binding properties of minimal oligosaccharides reveal a common heparan sulfate/dermatan sulfate-binding site in hepatocyte growth factor/scatter factor that can accommodate a wide variety of sulfation patterns. J Biol Chem 2009;284:6311–6321.
51. Friberg A, Corsini L, Mourao A, Sattler M. Structure and ligand binding of the extended tudor domain of *D. melanogaster*. J Mol Biol 2009;387:921–934.
52. Kukić P, Farrell D, Søndergaard CR, Bjarnadottir U, Bradley J, Pollastri G, Nielsen JE. Improving the analysis of NMR spectra tracking pH-induced conformational changes: removing artefacts of the electric field in the NMR chemical shift. Proteins 2010;78:971–984.
53. Parker LL, Houk AR, Jensen JH. Cooperative hydrogen bonding effects are key determinants of backbone amide proton chemical shifts in proteins. J Am Chem Soc 2006;128:9863–9872.
54. Bai G, Mo H, Shapiro M. NMR evaluation of adipocyte fatty acid binding protein (aP2) with *R*- and *S*-ibuprofen. Bioorg Med Chem 2008;16:4323–4330.